FZK contribution to the final IABAT report

C.H.M. Broeders, I. Broeders

Forschungszentrum Karlsruhe (FZK)

1 Introduction

The main FZK tasks defined in the IABAT program are spallation source optimization and comparison of accelerator driven systems (ADS) with critical fast and thermal reactors. The first step of the investigations was the implementation and qualification of suitable calculation methods and codes, especially for the description of the spallation processes and for the coupling of the external neutron source with the transport calculations for the subcritical reactor system. For the qualification of the calculation tools participation to several international benchmark investigations was very helpful. The applied high-energy codes could be validated by the participation to the NEA international code comparison of intermediate energy nuclear data [1]. For the validation of the burn-up and of the coupling of the spallation source with the subcritical reactor system, the IAEA ADS neutronic benchmark for lead cooled thorium/U^{233} fuel was a successful undertaking [2]. The results of the IAEA benchmark showed strong exponential power density increase towards the central spallation source. For this reason, at FZK the application of several distributed sources was investigated in some detail. Power density distributions and spallation product buildup in the target also were analyzed. The following sections give more information on these topics.

2 Development of codes and libraries

For the analysis of accelerator driven systems (ADS) the whole energy spectrum from several GeV down to thermal energies has to be covered. The traditional calculation tools for fission reactors only describe the energy range up to about 10 MeV for WIMS- and ABN-based libraries. Other multigroup libraries and also the special libraries for Monte Carlo calculations (e.g. MCNP) apply energies in the range of the evaluated data libraries like ENDF/B, usually being 20 MeV. For the higher energies special methods, data and codes had to be adapted from other research areas, e.g. from high-energy accelerator investigations. At FZK a 75 multigroup library for transport calculations with energies up to 50 MeV has been developed.
In figure 1 the basic flowchart for ADS investigations is shown. Three main components may be identified:

- Calculation of the neutron source with high energy transport codes
- Calculation of the steady state reactor with deterministic or Monte Carlo transport codes
- Burnup or depletion calculations

In the following sections these components will be discussed in some detail.

2.1 Development of codes

In connection with the ADS investigations, a number of developments have been accomplished for the different calculation stages.

2.1.1 High energy spallation calculations

The investigations started with the implementation and qualification of the HETC and MORSE modules from the HERMES [3] code system from the Jülich research center. The MORSE module was soon replaced by the more modern MCNP [4] code. Later on, the LAHET code system LCS [5] from Los Alamos, being an improved coupling of LAHET and MCNP4B was adopted and tested. Moreover, FZK is beta-tester of the new MCNPX [6] code system, in development at Los Alamos for ADS applications. In figures 2 and 3 some early results of proton source investigations are given. Figure 2 shows the distribution of spallation neutrons in an iron cylinder from the irradiation of a pencil beam source of protons with 1000 MeV energy. We may observe that for this beam type a concentrated forward-directed neutron distribution occurs. In figure 3 the spatial fission rate distributions in a subcritical system with thorium/U^{233} fuel is shown for three axial positions of the hitting point of a beam with proton energy 1500 MeV. We may observe that an optimal position between core boundary and mid-plane can be found to obtain symmetric power distributions around the core mid-plane.
All codes mentioned before are based on Monte Carlo simulations, both in the energy region for spallation and in the lower energy region for neutron transport.

2.1.2 Transport calculations

At FZK a strong effort was devoted to the qualification of the discrete ordinate code TWODANT [7] for the transport calculations below a cutoff energy of 10 to 50 MeV, in order to save significant amounts of computing times for simplified geometrical models. In figure 4 a comparison of TWODANT and MCNP results is shown for the radial power density distributions in two axial positions of the IAEA ADS benchmark (see also below). The TWODANT results were obtained on an IBM RS6000 workstation in about two hours of computing time, whereas the MCNP code needed several days on the same workstation. Obviously, for simplified geometrical models it is advantageous to apply deterministic codes. A number of design investigations have been carried out with multigroup diffusion calculations (see below).

2.1.3 Depletion calculations

A coupling of depletion calculations of the KAPROS/KARBUS [8] code system, developed for critical fast, epithermal and thermal reactors, with the codes HETC/LAHET and MCNP/ TWODANT was implemented and validated.
The KAPROS/KARBUS code system has been developed at FZK since many years. KAPROS [9] is a very flexible fully modular system consisting of a controller program and a large number of independent application modules. The system has been developed on an IBM mainframe computer. The first versions utilized the specific features of the computer environment at FZK with as a consequence that transferring to other computer environments was very problematic. In the past 10 years a portable version for workstations with UNIX operating systems has been redesigned and realized. The first applications were related to fast breeder reactors. In connection with investigations for tight light water reactors the treatment of upscattering in the thermal energy region and of the resonance absorption in the epithermal region has been significantly improved [8]. For fuel cycle studies a special module KARBUS was developed. The main tasks of KARBUS are:

- preparation and carrying out of one- to three-dimensional reactor calculations and
- the best estimate preparation of zone-dependent one-group cross sections for use in the depletion module BURNUP.

The module BURNUP is a KAPROS implementation of the program KORIGEN [10], the well-known FZK depletion code developed from the ORIGEN [11] code.

2.1.4 Coupling of the calculation steps

Figure 5 shows a more detailed overview of the actual system. However, it should be mentioned that the new MCNPX program combines LAHET and MCNP in one code. The application of MCNPX also may lead to some simplifications in the calculation scheme of figure 5. In general the code system KAPROS in conjunction with the powerful script languages of the UNIX operating systems are very flexible tools for the coupling of advanced computer codes.

2.2 Development of libraries

For the ADS investigations at FZK usually 69 group cross section libraries with the well-known WIMS [12] energy group structure are applied. The upper energy boundary of these libraries is 10 MeV. As a consequence the ADS investigations utilize the formalisms of the high-energy codes above 10 MeV. These formalisms are not well qualified in the energy range up to about 150 MeV. In order to be able to study the influences of these approximations with multigroup calculations, an extended library with energies up to 50 MeV and 6 additional groups above 10 MeV of the WIMS structure has been established.

2.2.1 Calculation procedures

The nuclear data processing at FZK is based on international standard data formats and calculation codes. The exchange of the basic data occurs with the ENDF/B [13] format. Group constants may be generated by the widely used processing code NJOY [14] in its latest version, at present a slightly modified version of NJOY97.95. For the data verification the ENDFB6 utilities version 6.11 [15] of CHECKR, LISTEF, PLOTEF and PSYCHE are available. For the KAPROS/KARBUS cross section processing an FZK-own development GRUBA/GRUCAL [16] is applied. Its main characteristics are [8]:

- the multigroup libraries have very flexible data storage on direct access files
- the data types and structures build a combination of the special features of fast and thermal reactor codes (upscattering, separate treatment of elastic, inelastic, n-2n, .. processes, isotope dependant fission spectrum matrices, etc)
- the cross section calculations are based on arbitrary rules on a so-called control-file
- data replacements may be easily realized by the so-called secondary input option
- a refined resonance treatment based on selfshielding tabulations (improved Bell-factor formalism) is applied
- the code system is well validated for a broad range of applications from heavy water moderated to lead cooled systems

For the reformatting of the NJOY-results to the special data storage modes a number of local programs are in use.

2.2.2 Development of a 75 group library with E_{max}=50 MeV

Since a few years extended nuclear data evaluations up to 50 MeV are established at FZK in a cooperation of the Project Nuclear Safety (ADS studies) and the Project Nuclear Fusion (IFMIF project [18]). The evaluation of the nuclear data files up to 50 MeV has been carried out by the Institute of Nuclear Power Engineering (INPE), Obninsk[19]. Above 20 MeV these cross-sections have been obtained from nuclear model calculations and from available ex-

perimental data. Most of the data below 20 MeV have been adopted from evaluated nuclear data libraries (ENDF/B-VI, JENDL3.2). The data for energies from 10^{-5}eV to 50 MeV have been made available in ENDF/B-6 format. From these efforts the following evaluations are available now:

- From the ADS project: O^{16}, Pb^{208}, Th^{232}, Pa^{233}, U^{233}, U^{235}, U^{238}, Pu^{239} and Pu^{240}.
- From the IFMIF project: Fe^{56}, Na^{23}, K^{39}, Cr^{52}, V^{51}, Si^{28} and C^{12}.

These evaluated data files with ENDF/B format have been processed by the NJOY code to produce adequate input files for the transport calculations. MCNP library generation is in progress within the IFMIF project. For the deterministic calculations, e.g. with the transport code TWODANT, multi-group libraries are required. The generation of a first version of a 75 group library with the Karlsruhe GRUBA format (69 WIMS energy group system, extended above 10 MeV with boundaries at 13.8, 15.0, 20.0, 27.1, 36.8 and 50 MeV) is completed. Some extensive comparisons of the basic data with the calculated group constants have been performed using the standard ENDF-based codes NJOY and PLOTEF and an old local plot program for comparisons of nuclear data from different origins. In figure 6 an example from the local plot code is shown for lead. The pointwise data for (n,?), (n,p) and (n,a) are compared with the multigroup library data type SCAPT, being the addition of the three reactions mentioned before. In figure 7 a plot generated by the NJOY code for the (n,2n) cross section of U^{235} is shown. The nuclear data processing code NJOY version 94.105 has been applied for the generation of these group constants. The group constants have been calculated for six temperatures: 300, 900, 1200, 1500, 2100 and 3000 K and for the seven values of the background cross section 10^{-3}, 10, 10^{1}, 10^{3}, 10^{4}, 10^{5}, 10^{10} barn. Neutron transfer matrices are given until Legendre order P_5.

The GRUBA system had to be extended to take into account reactions typical for energies above 10 MeV as e.g. (n,4n), (n,2n+a), (n,3n+a), (n,2n+p), (n,3n+p), (n,2p), (n,pd). As a typical test case a Pb^{208}-cylinder has been used with density and geometry corresponding to the lead target in the ADS neutronic benchmark [2], radius: 10 cm, height: 50 cm. In the model for the calculations a spatially homogeneous neutron source within a cylinder of radius 5 cm and height 10 cm in the center of the target was assumed. The energy dependence of the external source is similar to the one given in the benchmark specification. The highest neutron energy of the external neutron source (source 1) is 10 MeV; the lowest energy is 111 keV. Comparisons have been carried out for results obtained from calculations with TWODANT in S_{16}/P_3 approximation with the 69 group constant library that has been used for the benchmark calculations and with the new 75 group constants. Results for the total neutron leakage, the neutron flux density and for different reaction rates are shown in Table 1. The first 2 columns of Table 1 show calculations for Pb^{208}. The Pb^{208} data from INPE, Obninsk are based on ENDF/B-VI below 20 MeV. In order to eliminate from the comparison differences in nuclear data new Pb^{208} group constants in the 69 energy group structure have been recalculated. The deviations of the results obtained with the old and with the new group constant set are less than 1% except for a large deviation in the (n,a) reaction rate which is due to different data on ENDF/B-VI and on the Obninsk library. Columns 4 and 5 show calculations with the 75-group set. The energy of the external source neutrons (source 2) is between 50 MeV and 111 keV. Neutron flux density and reaction rates are given for two coarse energy groups: coarse group 1 between 10 MeV and 50 MeV and coarse group 2 between 10^{-5} MeV and 10 MeV. The contribution of neutrons above 10 MeV to the total neutron flux is about 6 %. The contribution of neutrons above 10 MeV to the total reaction rate, the reaction rates for (n,?), elastic and inelastic scattering is around 5 %. The contribution of neutrons above 10 MeV to the (n,2n) rate is about 93 %. For other threshold reactions (n, 3n), (n, p), (n, 2p), the contribution of neutrons above 10 MeV is more than 99 %. Column 3 of Table 1 shows that the capture

reaction rate of Pb^{208} in the spectrum of the lead cylinder is only about 20 % of the capture reaction rate of Pb^{207}.
As a first application of the new 75 group constant set for a reactor, the fresh core of the ADS neutronic benchmark [2] has been recalculated. The calculations have been carried out with TWODANT in S_8/P_3 approximation. Table 2 shows the results for K_{eff} and K_{source} for different U^{233} enrichments of the fuel. The U^{233} enrichment that is necessary to obtain K_{eff}=0.96 is lower (8.722 at %), when the new group constant set is applied. This is mainly due to the difference in the basic nuclear data below 10 MeV. On the Obninsk library the data for U^{233} and Th^{232} below 20 MeV are mainly from JENDL-3.2, most of the data for Pb^{208} below 20 MeV are from ENDF/B-VI. In order to eliminate most of the differences in the data the cross sections for U^{233} and Th^{232} in the 69 group constant library were replaced by data from JENDL-3.2 and the cross sections of Pb^{208} were replaced by group constants obtained from ENDF/B-VI. In Table 2 the 69 group constant library with the replacements discussed above is called modified 69 group constant set. The results for Keff calculated with this modified 69 group constant set and with the 75-group constant set differ by about 1 % as is shown in table 2. For K_{source} a similar difference is found.

3. ADS system studies

ADS system studies were started as soon as reliable qualified calculation tools were available. After some preliminary studies of the capabilities of ADS for the incineration of plutonium, minor actinides and long lived fission products [20], the participation to the IAEA ADS benchmark lead to a number of program developments and resulted in insights of large interest. Especially the power distribution towards the central neutron source proved to be unsatisfactory with radial form factors varying from about 2.5 to nearly 4 (see below). In order to improve these unacceptable characteristics at FZK an ADS with up to six distributed neutron sources was proposed and investigated. On the basis of this multi source design a number of more detailed investigations related to the incineration of plutonium and minor actinides have been performed. The next sections describe these issues in some more detail.

3.1 Applied codes and models

A more detailed description of the codes may be found in section 2.1. For the IAEA ADS benchmark investigations a two-dimensional cylindrical model was defined. Comparisons of Monte Carlo calculations with MCNP and deterministic calculations with TWODANT confirmed that for this simplified geometrical model the results of these codes are in satisfactory agreement. For this reason the required depletion calculations were carried out with the much faster deterministic transport code TWODANT. The investigations of the multi-source systems were performed with the diffusion code D3E [21] with triangular geometry, developed at FZK. Some comparison calculations with the widely used CITATION [22] code showed good agreement. For the depletion calculations two different options of the KARBUS system have been applied:

- Direct depletion calculations with the module BURNUP.

After each time-step and in each reactor zone mean one-group cross sections are prepared on the basis of mean 69 group fluxes and shielded 69 group cross sections. These one-group cross sections are applied in the module BURNUP, derived from the (K)ORIGEN code [10].

- Application of pre-calculated burn-up-dependent macroscopic cross sections with the core simulation program ARCOSI [8].

For each fuel composition a burn-up calculation with sufficiently detailed time-steps and with burn-up up to about 150 MWD/THM is performed on the basis of 69 group cross sections.

The 69 group burn-up dependent cross sections are collapsed to 4 group data, using weighting spectra based on fundamental mode calculations. This procedure has been developed and validated for tight light water reactor studies [8] and applies the B^{10} content of the coolant as an additional parameter. The resulting 4 group macroscopic cross sections are stored on a special library and may be utilized by the core-simulator code ARCOSI. For the fast spectrum ADS applications with thorium and minor actinide fuel the procedure of the 4-group library generation had to be modified. It was found, that for fuels containing isotopes with relatively short decay times like Pa^{233} (27 days) and Cm^{242} (162.8 days) the reactivity of the system is sensitive to the flux level in the fuel. Instead of the B^{10} parameterization, the power density in the fuel is varied for the generation of the 4 group libraries.

3.2 IAEA ADS benchmark (Th-U^{233} based energy amplifier)

In 1996 the IAEA initiated an international ADS benchmark based on a proposal of Rubbia et.al. [23] for an energy amplifier with a power of 1500 MW_{th} and based on Th-U^{233} fuel in hexagonal fuel assemblies and with lead coolant. For the FZK contribution [24] the calculations of the neutron-flux density spectra and of reaction rates (total fission reaction rate, fission reaction rates for individual isotopes) have been carried out with the transport code TWODANT in S_4/P_1 approximation. For the calculations multigroup cross sections of a recent 69-energy group constant library have been used (G69P1V03). The nuclear database of most of these group constants is KEDAK-IV [25], some of the group constants have been newly calculated from more recent libraries: e.g. U^{233} from ENDF/B-VI and Th^{232} from the JEF-2.2 library. In the calculations the temperature of the fuel was 1200K, the temperature of lead and steel was 900K. The neutron source provided with the benchmark data has been transformed to the 69 energy group structure of our group constant set in such a way that for each energy group the number of neutrons per eV was conserved. Table 3 shows the initial U^{233} enrichments for the required different K_{eff}-values.

3.2.1 Burnup behavior

An important objective of the IAEA ADS benchmark was the determination of the time-dependence of the reactivity of the sub-critical reactor system. In the benchmark specifications the power-level and the time-steps are specified in detail. The cylindrical geometry model-specification contains 5 zones: lead, inner core, outer core, radial reflector and axial reflector. For the burn-up calculations each fuel zone was subdivided into 3 radial and 3 axial sub-zones, leading to a TWODANT (R-Z)-model with 22 zones. During the analysis of the results it pointed out that some other benchmark solutions were based on burn-up calculations without sub-division of the fuel zones. For that reason a consistent calculation without sub-division was carried out, leading to a TWODANT (R-Z)-model with 7 zones. In figure 8 FZK results for the time-dependence of the reactivity is shown. These results are in good agreement with solutions of other participants. We may observe that for the case K_{eff}=0.96 the influence of the sub-division of the fuel zones is remarkable.

3.2.2 Power distributions

The technical feasibility of an ADS is strongly influenced by the power density distribution in the system. So, another important issue of the IAEA ADS benchmark investigation was the comparison of the radial power distributions for the different sub-criticality levels. In general

the agreement between the solutions of the participants was good. In figure 9 the radial power density distribution in the mid-plane of the reactor system is shown. Also the radial form-factors, defined as maximum-to-mean power density ratio, are given. We may observe that the form-factor strongly increases with decreasing reactivity of the system. For a sub-critical system the flux–distribution towards the neutron source tends to an exponential shape. For a central neutron source this is in contrast to the smooth shape to the center of a critical system. The values obtained in the benchmark configuration are not acceptable in large power systems. As a consequence of these observations at FZK a considerable effort was devoted to improve the power-density distribution. Although the typical solution for fast critical reactors to increase the fissile enrichment in two to three radial zones also leads to improvements in an ADS, a better solution seems to be to apply more than one spallation source in the system. Exploratory investigations were carried with two to six non-central spallation sources. In the figures 10, 11 and 12 examples of power density distributions in an ADS with Th/U^{233} fuel and with six, three and one neutron sources are shown. In the next section more detailed information is given for multi-source systems for the incineration of plutonium and minor actinides.

3.3 Plutonium and minor actinide burner

At FZK a main objective of the ADS investigations is to analyze its characteristics for closing the back-end of the nuclear fuel cycle. An important parameter in these studies is the possible incineration rate of plutonium, minor actinides and long-lived fission products. In the next sections two cases for different fuels are presented. Both cases are based on discharged fuel from pressurized water reactors (PWR) with a mean burn-up of 50.000 MWD/THM. Seven years cooling time and three years fabrication time are assumed for the ex-core times

- All heavy metal fuel isotopes are kept together. The required criticality of about 0.98 is obtained by mixing with thorium.
- Plutonium and all minor actinides together are kept in two separate stocks. In this case no other fuel is added. The criticality of about 0.98 is obtained by mixing with zirconium.

3.3.1 Choice of the number of proton beams

Obviously, power density distributions in accelerator driven sub-critical systems may be improved if instead of one central target several targets are distributed over the core. It is also clear that an increased number of proton sources makes the system technically more complicated. In the first FZK application a number of six beams quite near to the core boundary was chosen (see figure 10). With this arrangement acceptable power factors could be obtained. However, for this system the leakage of spallation neutrons is considerable and the reactivity decreases significantly compared to a system with one central proton source. Therefore the sources were moved to the center of the core and satisfactory power density distributions could be found with three proton beams (see figure 11). For this arrangement only small influences of leakage increase may be observed. The more systematic investigations in reference [26] confirm that the choice of three beams may be a good compromise concerning power density distributions and system complexity. ADS cores with three proton beams and two types of fuel as specified before have been investigated in some more detail.

3.3.2 Incineration in a thorium based system

In a first series of investigations the incineration of a mixture of not-separated heavy metals from spent LWR-fuel with 50.000 MWD/THM mean discharge burn-up was considered. The desired sub-criticality was obtained by mixing this fuel with thorium. In table 4 the weights and isotopic compositions at begin of life are given.
For this fuel burn-up data was prepared up till 140.000 MWD/THM. The reactor core was described by a full 3-D hexagonal geometry with 16 axial layers. Burn-up simulations with 1084 regions with the program ARCOSI were performed until in one region of the model the maximum burn-up of 140.000 MWD/THM is exceeded.

3.3.3 Incineration in a thorium- and uranium-free system

In a further series of investigations the incineration of a mixture of separated stocks of plutonium and minor actinides from spent LWR-fuel with 50.000 MWD/THM mean discharge burn-up was considered. The desired sub-criticality was obtained by mixing these fuel components in a proper way and with about 60% zirconium as matrix material. In table 5 the weights and isotopic compositions of the fuel at begin of life are given. This fuel is very advanced and problems might arise for manufacturing and maintaining. The present results only give information on the characteristics from the neutronic point of view. For this fuel the same burn-up simulations with the program ARCOSI as in the preceding section were performed.

3.3.4 Results.

In figure 13 the burn-up dependence of the reactivity of the systems of section 3.3.2 and 3.3.3 is shown. For the Th/Pu-MA fuel two different arrangements of the proton sources are investigated, identified by the fuel assembly numbers (20,26,32) and (38,46,54). Obviously, the second case with proton sources somewhat more to the outer boundary of the core is more favorable: the reactivity is slightly higher and the upper limit of the fuel burn-up is reached later, indicating better power density distributions. The Th/Pu-MA results also show the strong influence of the build-up of U^{233} from Th^{232} captures with a reactivity increase of about 6% during burn-up. The typical reactivity decrease due to the Pa^{233} build-up during the first 50 to 100 days also may be observed. On the other hand, the Th-free fuel leads to a very flat reactivity behavior. In figure 14 the change rates in (kg/MWe.Year) of uranium and plutonium in the Th/Pu-MA system are shown. A load-factor 1. and a system-efficiency of 40% are assumed for the normalization to (Mwe.Year). It may be observed that in this design the uranium production exceeds the plutonium incineration. The change rates for minor actinides are given in figure 15 for both cases. The change rates for the minor actinides are small in the Th/Pu-MA system. In the second minor actinide burner system (MAB) the incineration rates of americium and neptunium are much better. Curium is always produced (changes are always positive). In the MAB system a considerable amount of Pu^{238} with half-life 87.7 years is produced

4. Target studies

A major area of investigations for accelerator driven systems is related to the spallation target problems. In the next sections investigations on the energy deposition in spallation targets and on the significance of spallation products will be discussed in some detail.

4.1 Applied codes and models

A more detailed description of the codes may be found in section 2.1. Most calculations were performed with the LAHET code system LCS. Some of the investigations have also been carried out with the beta test version 2.1.5 of MCNPX. In figure 16 the good agreement between LCS and MCNPX is demonstrated for the neutron spectrum from 600 MeV protons in a spallation target. For the core calculations the geometry specifications of the IAEA ADS benchmark mentioned before usually have been applied. For the investigation of the energy deposition in the spallation target a detailed MCNP model was used.

4.2 Energy deposition

The spallation target and the beam window are very important components of an accelerator-driven system (ADS). In this area high power densities may occur and reliable calculation methods are required for the energy deposition in order to be able to design the heat removal facilities. The main goal of the investigation (see also reference [27]) is the determination of the spatial distribution of the energy deposition in the target. Most of the calculations have been carried out with the LAHET Code System (LCS). For the nuclear model parameters that have to be chosen by the input of LAHET the default values are used, with the only exception that a preequilibrium phase following the intranuclear cascade was specified. For the calculations the following models and methods are used (in parentheses the corresponding LCS input variables):

- The Bertini model for the simulation of the intranuclear cascade (IEXISA=0)
- A preequilibrium model following the intranuclear cascade (IPREQ=1)
- The RAL (Rutherford and Appleton Laboratories) evaporation-fission model (IEVAP=0)
- For light nuclei (A<18) the evaporation model is replaced by the Fermi breakup model (IFBRK=1)
- The Gilbert-Cameron-Cook-Ignatyuk level density model (ILVDEN=0)
- The neutron elastic scattering data file ELSTIN which is part of the LCS system (NOELAS=23)
- The nucleon-pion transport option (NBERTP=1)

(See [29] and references given there for more details)

In figure 17 a global layout of the (R-Z) model for the core calculations, based on the IAEA ADS benchmark, is shown. Figure 18 gives the geometry model of the target, based on preliminary design considerations at FZK [28]. In figure 19 a close-up view in the vicinity of the window is shown. The shadowed area indicates the arrangement and the shape of the intensity of the proton beam. The proton range in different candidate target materials as a function of the proton energy is given in figure 20. It may be observed that the differences are remarkable between lead and HT9 steel on the one hand, and tungsten and rhenium on the other hand. The energy deposition in the target strongly depends on the characteristics of the proton beam. For the arrangement of figure18 a detailed analysis was performed. The final result is shown in the power density distribution in figure 21. We may clearly recognize the shape of the proton beam intensity.

4.3 Spallation product analysis

During the irradiation of an ADS-target with protons a large number of spallation products are produced. Most of these spallation products have short lifetimes and have no significant impact on the behavior of the system. However, a considerable number of spallation products or

their successors have longer lifetimes and must be taken into account with respect to the criticality of the system and to the consequences for the back-end of the system. Recently a Russian study has been published with a comparison of long-lived residual activity characteristics of liquid metal coolants for advanced nuclear energy systems [30]. In this reference the impact of Pb^{205} with lead coolant and of Bi^{210m} with lead-bismuth coolant is pointed out. At FZK the significance of spallation products in a fast spectrum ADS has been investigated in some detail [31]. The study is performed for a lead-cooled sub-critical energy amplifier system, similar to the proposal of Rubbia [23]. It has been shown that in a fast spectrum the neutron absorption in the spallation products only presents a weak competition to the nuclear decay as long as the half-life is smaller than about 30 days. So tabulations have been made for isotopes with decay times larger than 30 days. In order to reduce the amount of output the printouts are restricted to abundance above 1%. These tabulations are based on decay calculations without competition of neutron interactions utilizing an extensive decay-list of some 3000 isotopes and meta-stable states, compiled in conjunction with the investigations in reference [32]. The most important spallation products in a lead target are summarized in table 6, including half-life, yield per proton and availability on evaluated nuclear data files. We may observe a quite large number of missing isotopes on the evaluated data files, e.g. Pb^{205} with high yield and long half-life. In table 7 one-group cross sections of important spallation products in the inner core of a Rubbia-type energy amplifier are compared. The one-group cross sections have been calculated with the processing code NJOY, using the different evaluated data libraries ENDF/B-6, JENDL-3.2 and JEF-2.2. Also given are the corresponding fast spectrum values on the KORIGEN library. The differences between the one-group cross sections from different origins are remarkable, both for KORIGEN and the other calculated values. For the impact of the spallation products on the reactivity of the fast spectrum ADS an educated guess leads to about 1% of the fission product contribution if the sub-criticality level of the system is low (about 0.75). For slightly sub-critical systems the influence may be neglected.

5. Comparison of critical and sub-critical systems

A first systematic discussion of the different characteristics of possible critical reactor systems (CRS) and accelerator driven systems (ADS) is given in reference [33]. It is proposed only to compare similar systems, based on the same design principles. Comparisons concerning applied calculation procedures, flux and power distributions, power level control, burn-up behavior, incineration potential, aspects of dynamics and accident analysis and possible future R&D-work related to fast neutron spectrum designs of CRS and ADS are discussed in this reference. The main arguments for the ADS concepts are usually the improved safety, compared to CRS. Indeed, some ADS objectives hardly may be realized with CRS, e.g. incineration of larger amounts of long-lived fission products or of heavy fuel isotopes with unfavorable properties for the dynamics behavior (delayed neutron fractions, coolant density and fuel temperature reactivity coefficients, etc.). A comparison of similar fast spectrum CRS and ADS designs shows an improvement of the safety characteristics of an ADS, caused by the lower required fissile enrichments. However, it is not clear that in fast spectrum ADS recriticality during core damaging accidents can be avoided in all circumstances. In the case core damaging accidents with recriticality cannot be excluded, reconsidering thermal ADS may be a more suitable solution. Finally one has to keep in mind that both **critical and sub-critical burner reactors** only may be run if reprocessing plants with adequate capacity for the fuel cycles of interest are realized.

6. References

[1] D. Filges, P.Nagel, R.D. Neef, editors
OECD Thick Target Benchmark for Lead and Tungsten
Report NSC/DOC(95)2 (1995)

[2] I. Slessarev, A. Tschistiakov,
IAEA-ADS BENCHMARK (Stage 1)
RESULTS and ANALYSIS
TCM-Meeting, Madrid, 17-19 September 1997

[3] P. Cloth, D. Filges, R.D. Neef, G. Sterzenbach, Ch. Reul, T.W. Armstrong,
B.L. Colborn, B. Anders, H. Brückmann
HERMES
A Monte Carlo Program System for Beam-Materials Interaction Studies
Jül-2203, May 1988

[4] J.F. Briesmeister, editor
MCNP-A General Monte Carlo N-Particle Transport Code, Version 4B
LA-12625-M, Version 4B Issued: March 1997

[5] R.E. Prael and H. Lichtenstein
User Guide to LCS: The LAHET Code System
LA-UR-89-3014 Revised September 15, 1989
and
R.E. Prael
Upgrade Package for LCS with LAHET2.7
LA-UR-97-4981 December 1, 1997

[6] H.G. Hughes, R.E. Prael, R.C. Little,
MCNPX - The LAHET/MCNP Code Merger
LA-UR-97-4891, XTM-RN(U)97-012, April 22, 1997
and
H.G. Hughes,K.J. Adams,M.B. Chadwick, J.C. Comly, S.C. Frankle,
J.S. Hendricks, R.C. Little, R.E. Prael, L.S. Waters,, and P.G. Young,Jr.
Status of the MCNP™ / LCS™ Merger Project
Proceedings of the Radiation Protection and Shielding Topical Conference
Nashville, Tennessee, April 19-23,1998

[7] R.E. Alcouffe, F.W. Brinkley, D.R. Marr, R.D. O'Dell,
Users Guide for TWODANT: A Code-Package for Two-Dimensional,
Diffusion-Accelerated, Neutral Particle Transport,
LA-10049-M, Rev. 1, Manual, October 1984, Revised February 1990

[8] C.H.M. Broeders
Entwicklungsarbeiten für die neutronernphysikalische Auslegung von
Fortschrittlichen Druckwasserreaktoren (FDWR) mit kompakten
Dreiecksgittern in hexagonalen Brennelementen
KfK 5072 (August 1992)

[9] H. Bachmann, G. Buckel, W. Hoebel, S. Kleinheins
The Modular System KAPROS for Efficient Management of Complex Reactor Calculations",
Proceedings Conference Computational Methods in Nuclear Energy, Charleston, CONF-750413 (1975)

[10] U. Fischer, H.W. Wiese,
Verbesserte konsistente Berechnung des nuklearen Inventars abgebrannter DWR-Brennstoffe auf der Basis von Zell-Abbrand-Verfahren mit KORIGEN,
KfK 3014 (1983)

[11] M.J. Bell,
ORIGEN- The ORNL Isotope Generation and Depletion Code,
ORNL-4628 UC-32 (1973)

[12] J.R. Askew, F.J. Fayers, P.B. Kemshell,
A General Description of the Lattice Code WIMS,
Journal of British Nuclear Energy Society, 5,564 (1966)

[13] P.F. Rose, C.L. Dunford, editors
ENDF-102
Data Formats and Procedures for the evaluated nuclear data file ENDF-6
BNL-NCS-44945 (1990)

[14] R.E. MacFarlane et. al.
Documentation for PSR-368/NJOY97.0 Code Package (1998)

[15] C.L. Dunford,
ENDF Utility Codes Release 6.10
Code Manual (1995)

[16] D. Woll,
GRUCAL, Ein Programmsystem zur Berechnung makroskopischer Gruppenkonstanten,
KFK 2108 (1975)

[17] C. Broeders, I. Broeders,
Generation of a Group Constant Library for Neutron Energy until 50MeV, Tests and Applications
FZKA 6126, pages 580 – 586, (1998)

[18] M. Martone, editor
IFMIF Conceptual Design Activity, Final Report
ENEA Frascati Report RT/ERG/FUS/96/11 (1996)

[19] Yu.A. Korovin, A.Yu. Konobeyev, P.E. Pereslavtsev, A.Yu. Stankovsky,
C. Broeders, I. Broeders, U. Fischer, U. v.Möllendorff, P. Wilson, D. Woll
Evaluation and Test of nuclear Data for Investigation of Neutron Transport,
Radiation Damage and Processes of Activation and Transmutation in
Materials Irradiated by Intermediate and High Energy Particles
G. Reffo, editor
International Conference on Nuclear Data for Science and Technology,
Trieste, May 19-24, 1997.

[20] I. Broeders, C.H.M. Broeders
Implementation, Development, Validation and First Applications
of Different Code Chains for the Investigation of
Accelerator-Driven Transmutation
Proceedings of ICENES-96 ,Obninsk (1996)

[21] B. Stehle,
D3D und D3E, Zweige eines FORTRAN-Programms zur Lösung der
stationären dreidimensionalen Multigruppen Neutronendiffusionsgleichungen
in Rechteck-, Zylinder- und Dreieckgeometrie,
KfK-4764 (1991)

[22] T.B. Fowler, D.R. Vondy,
Nuclear Reactor Core Analysis Code: CITATION,
ORNL-TM-2496. Rev. 1 (1970)

[23] C. Rubbia, J.A. Rubio, S. Buono, F. Carminati, N. Fietier, J. Galvez, C. Geles,
Y.Kadi, R. Klapisch, P. Mandrillon, J.P. Revol and Ch. Roche,
Conceptual Design of a Fast Neutron Operated High Power Energy Amplifier
CERN/AT/95-44(ET) (1995)

[24] C.Broeders, I.Broeders
Calculations for the IAEA coordinated ADS neutronic benchmark
FZKA 5963 ,pages 464 – 472, (1997)

[25] B. Goel, B. Krieg,
Status of the Nuclear Data Library KEDAK4,
KfK 3838 (1984)

[26] R. Dagan, C.H.M. Broeders
Optimization of Multiple Source System for ADS
20. Conference of Nuclear Societies in Israel (1999)

[27] C. Broeders, I. Broeders,
Calculations of the Energy Deposition in the Target of an ADS
FZKA 6300 ,pages 663 – 672, (1999)

[28] X. Cheng, J.U.Knebel,
Private communication (1999)

[29] R.E. Prael,
A Review of Physics Models in the LAHET™ Code
LA-UR-94-1817
and in
Intermediate Energy Nuclear Data: Models and Codes
Proceedings of a Specialist's meeting Issy-Les-Moulineaux (France)
OECD Documents 30 May-1 June 1994

[30] V.I. Oussanov, D.V. Pankratov, E.P. Popov, P.I. Markelov,
L.D. Riabaya, S.V. Zabrodskaya,
Long-lived Residual Activity Characteristics of some Liquid Metal Coolants
For Advanced Nuclear Energy Systems
Proceedings of GLOBAL-99 Conference, Jackson, WY, USA (1999)

[31] M. Segev, C. Broeders, I. Broeders
Significance of Spallation Products in a Fast Spectrum ADS
Forschungszentrum Karlsruhe Internal report January 1999

[32] M. Segev, PROSDOR – An IBM-3090 Based Semi-Automated Procedure
Linking HERMES MCNPand KORIGEN for the Burnup Analysis of
Accelerator Driven Cores
KfK-5328 (1994)

[33] C.H.M. Broeders,
A Comparison of Some Neutronics Characteristics of Critical Reactors and
Accelerator Driven Subcritical Sytems
Proceedings of Fifth International Exchange Meeting Mol, Belgium (1998)

Lead Target with external source TWODANT calculations in S_8/P_3 approximation comparison of neutron flux densities and reaction rates from 69 and 75 group constant libraries					
case	75 groups source 1 Pb^{208}	69 groups source 1 Pb^{208} $E \leq 10MeV$	69 groups source 1 Pb^{207}	75 groups source 2 Pb^{208} $E \leq$ 10MeV	$E \geq$ 10MeV
net leakage	1.016E+0	1.016E+0	1.021E+0	1.195E+0	1.195E+0
neutron flux	2.131E+1	2.119E+1	2.240E+1	2.281E+1	1.523E+0
reaction rates					
total	3.873E+0	3.865E+0	4.342E+0	4.142E+0	2.478E-1
capture	4.236E-4	4.217E-4	1.850E-3	4.332E-4	7.601E-4
(n,γ)	4.232E-4			4.330E-4	1.475E-5
(n,α)	4.147E-7	1.512E-6		1.973E-7	2.042E-4
(n, p)	4.978E-8	4.969E-8		8.350E-9	4.987E-4
(n, 2p)					4.789E-5
(n, p d)					1.053E-5
elastic	3.648E+0	3.637E+0	3.961E+0	3.999E+0	1.414E-1
inelastic	2.098E-1	2.111E-1	3.564E-1	1.400E-1	1.017E-2
(n,2n)	1.643E-2	1.641E-2	2.292E-2	2.594E-3	3.618E-2
(n,3n)	0.0	0.0	0.0	0.0	2.393E-2
(n,4n)	0.0	0.0	0.0	0.0	2.156E-2

Table 1: TWODANT results for lead target with 69 and 75 group constant libraries.

ADS Neutronic Benchmark k_{eff} and k_{source} calculated with different group constant libraries		
A. critiality calculations		
U^{233} enrichment	k_{eff} 75 energy groups from Obninsk data (0-50 MeV)	 69 energy groups modified set (0-10 MeV)
9.68	1.0243136	1.01362481
8.72	.96000698	.94995146
B. source calculations		
U^{233} enrichment atom percent	k_{source} 75 energy groups source up to 50MeV	 69 energy groups modified set source up to 10 MeV
8.72	$.97643827^{(1)}$ $.97158054^{(2)}$	.96300135

$$k_{source}^{(1)} = \frac{R(\nu \cdot fiss)+R(n,2n)+R(n,2n+x)+2\cdot[R(n,3n)+R(n,3n+x)]+3R(n,4n)}{L+R(abs)}$$

$$k_{source}^{(2)} = \frac{R(\nu \cdot fiss)+R(n,2n)}{L+R(abs)}$$

R: reaction rate

(n,2n+x): $(n,2n+p)+(n,2n+\alpha)+(n,2n+2\alpha)$

(n,3n+x): $(n,3n+p)+(n,3n+\alpha)$

L: net leakage

Table 2: TWODANT results for ADS benchmark with 69 and 75 group constants.

Initial enrichment of U^{233} in regions 1 and 2	
Enrichment=relation of atom number densities: $U^{233}/(U^{233}+Th^{232})$	
$k_{eff}(BOL)$	$U^{233}/(U^{233}+Th^{232})$
0.98	10 at % $U^{233}/(Th^{232}+U^{233})$
0.96	9.68 at %
0.94	9.36 at %

Table 3: Initial enrichments of U^{233} for the different K_{eff}-values of the IAEA ADS benchmark

Fuel inventory ADS with Th/TRU fuel

Heavy metal from PWR discharged fuel with
mean burnup 50.000 MWD/THM
7 yrs cooling, 3 yrs fabrication time
(weights in kg)

Material	Core	Reflector	Total
Thorium	12106.0	4735.8	16841.8
Neptunium	140.2	0	140.2
Plutonium	2343.0	0	2343.0
Americium	78.2	0	78.2
Curium	21.8	0	21.8

Plutonium-vector (weight%):

Pu^{238}	Pu^{239}	Pu^{240}	Pu^{241}	Pu^{242}
2.7	53.7	23.8	12.3	7.5

Americium-vector (weight%):

Am^{241}	Am^{243}
65.3	34.7

Table 4: Fuel inventory specifications of an ADS core with Th/Pu-MA fuel

Fuel inventory ADS with TRU/Zr fuel

Heavy metal from PWR discharged fuel with
mean burnup 50.000 MWD/THM
7 yrs cooling, 3 yrs fabrication time
(weights in kg)

Material	Core	Reflector	Total
Thorium	-	-	-
Neptunium	3002.4	0	3002.4
Plutonium	2838.4	0	2838.4
Americium	1675.4	0	1675.4
Curium	466.0	0	466.0

Plutonium-vector (weight%):

Pu^{238}	Pu^{239}	Pu^{240}	Pu^{241}	Pu^{242}
2.7	53.7	23.8	12.3	7.5

Americium-vector (weight%):

Am^{241}	Am^{243}
65.3	34.7

Table 5: Fuel inventory specifications of an ADS core with Pu/MA/Zr fuel

SPALLATION PRODUCTS IN THE LEAD TARGET OF THE RUBBIA ADS CONCEPT
The list is shortened to include those elements for which
a: half-life > 30 days
b: relative abundance in the target > 1.0%

isotope	half life	yield per proton	basic neutron xsection data available in compilation					
			-1-	-2-	-3-	-4-	-5-	-6-
82 Pb 206	s	0.454	+		+	+		+
82 Pb 207	s	0.252	+		+	+		+
82 Pb 205	1.5+07 a	0.228						
82 Pb 204	1.4+17 a	0.150	+					+
81 Tl 203	s	0.143						
82 Pb 208	s	0.139	+		+	+		+
80 Hg 201	s	0.079						
80 Hg 200	s	0.077						
80 Hg 199	s	0.070						
82 Pb 202	~3 +05 a	0.064						
79 Au 195	183 d	0.062						
80 Hg 203	46.6 d	0.060						
80 Hg 198	s	0.059						
81 Tl 205	s	0.054						
79 Au 197	s	0.052	+	+	+	+	+	
80 Hg 196	s	0.042						
80 Hg 202	s	0.039						
78 Pt 193	~ 50 a	0.034						
81 Tl 203	s	0.033						
76 Os 186	2.0+15 a	0.030						
80 Hg 194	367 a	0.029						

legend
------
1 - brond22
2 - cendl21
3 - endfb6
4 - endfb64
5 - jef22
6 - jendl32

Table 6: Spallation products in the lead target of an ADS

EFFECTIVE ONE-GROUP CROSS SECTIONS OF SOME SPALLATION PRODUCTS
IN THE INNER-CORE OF THE RUBBIA ADS CONCEPT

(the list is arbitrarily shortened to include those elements for which)
(half-life > 30 days)
(relative abundancy in the inner-core > 1.0%)

					cross sections (barns)			
						NJOY-generated ; collapsed on the flux-spectrum		
					KORIGEN	of the Rubbia-concept inner-core		
	half	yield			LIBRARIES			
isotope	life	per	reaction			endfb6	jendl32	jef22
	days	proton	type					
6 C	12	s	0.0293	n,gamma	1.56 -3	2.65 -6	1.79 -5	2.65 -6
				n,alpha	(both)	1.22 -2	1.34 -2	1.31 -2
7 C	15	s	0.0140	n,gamma		1.19 -5	3.70 -7	3.70 -7
				n,alpha		3.04 -4	2.94 -4	2.94 -4
8 O	16	s	0.0220	n,gamma	6.00 -4	1.34 -7	5.35 -5	1.34 -7
				n,alpha	(both)	1.30 -2	2.32 -2	1.30 -2
24 Cr	52	s	0.0113	n,gamma	1.53 -3	6.16 -3	6.36 -3	6.41 -3
				n,alpha	(both)	4.85 -5	4.98 -4	4.74 -4
25 Mn	54	312	0.0133	n,gamma				
				n,alpha				
25 Mn	55	s	0.0170	n,gamma	1.93 -2	3.83 -2	3.83 -2	5.34 -2
				n,alpha	(both)	2.60 -5	2.60 -5	2.24 -5
26 Fe	54	s	0.0107	n,gamma				
				n,alpha				
26 Fe	55	986	0.0203	n,gamma				
				n,alpha				
26 Fe	56	s	0.0220	n,gamma	1.01 -2	8.43 -3	9.28 -3	8.04 -3
				n,alpha	(both)	1.44 -4	1.29 -4	6.42 -4
80 Hg	200	s	0.0143	n,gamma				
80 Hg	201	s	0.0157	n,gamma				
81 Tl	203	s	0.0337	n,gamma				
82 Pb	202	1.1+8	0.0180	n,gamma				
82 Pb	204	5.+19	0.0473	n,gamma			6.54 -2	

82 Pb 205	5.5+9	0.0640	n,gamma				
82 Pb 206	s	0.1370	n,gamma		1.05 -2	8.80 -3	
82 Pb 207	s	0.0791	n,gamma		7.61 -3	5.95 -3	
82 Pb 208	s	0.0458	n,gamma		7.66 -4	6.55 -4	
90 Th 228	697	0.0149	n,gamma	4.00 -1		3.62 -1	
			n,fiss	4.00 -1		1.59 -2	
90 Th 229	2.7+6	0.0227	n,gamma	4.00 -1		1.197	
			n,fiss	3.00		7.92 -1	
90 Th 230	2.8+7	0.0220	n,gamma	4.00 -1	1.97 -1	3.80 -1	1.97 -1
			n,fiss	4.40 -1	2.81 -2	7.01 -2	2.81 -2
90 Th 232	5.+12	0.0164	n,gamma	4.44 -1	3.64 -1	3.48 -1	3.81 -1
			n,fiss	1.37 -2	2.84 -2	2.53 -2	6.33 -2
91 Pa 231	1.2+7	0.0157	n,gamma	8.00 -1	1.01	1.37	1.01
			n,fiss	3.83 -1	1.79 -1	1.49 -1	1.79 –1

Table 7: Effective one-group cross sections for selected spallation products in a fast neutron spectrum

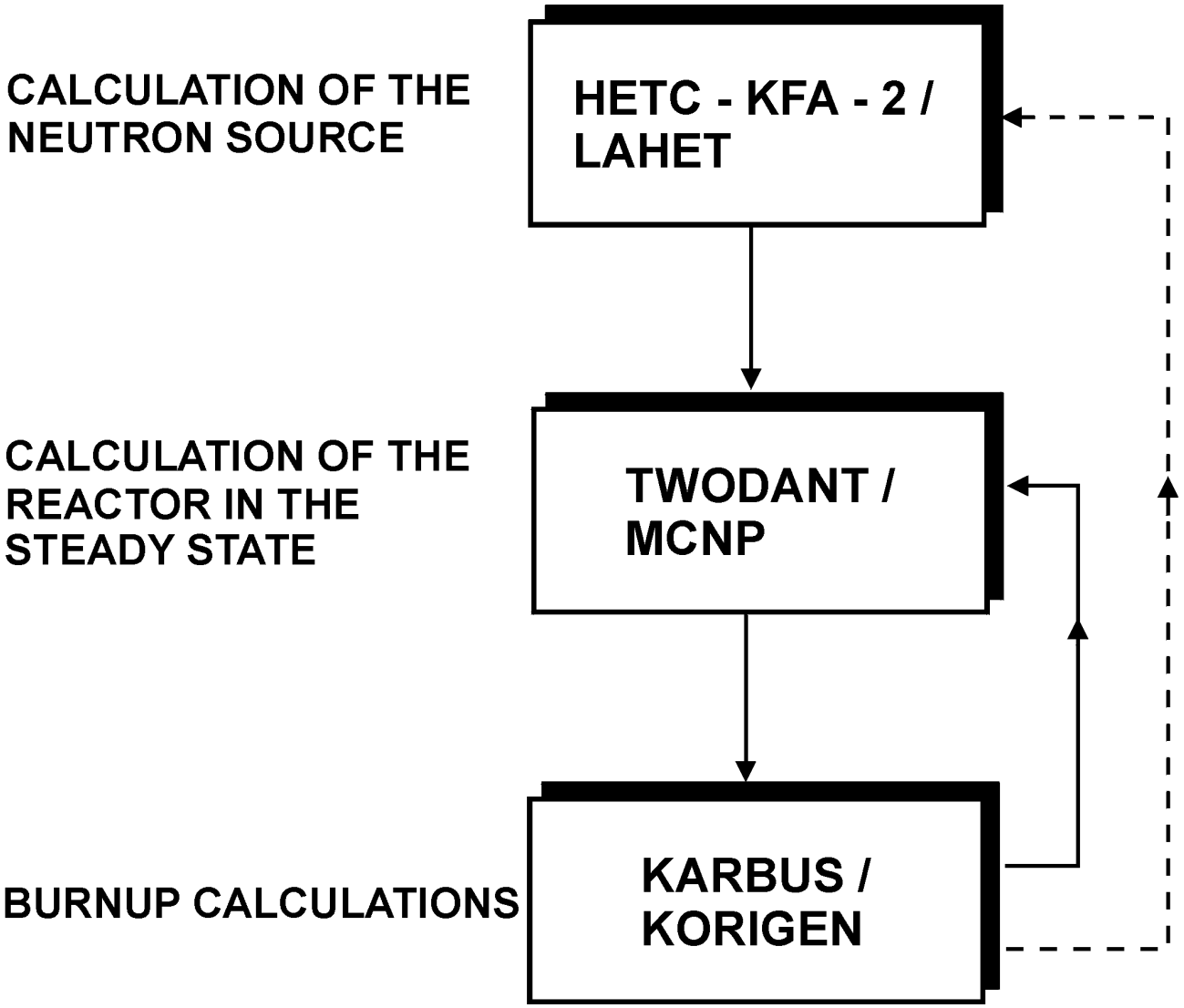

Figure 1: Simplified flowchart for a complete ADS calculation

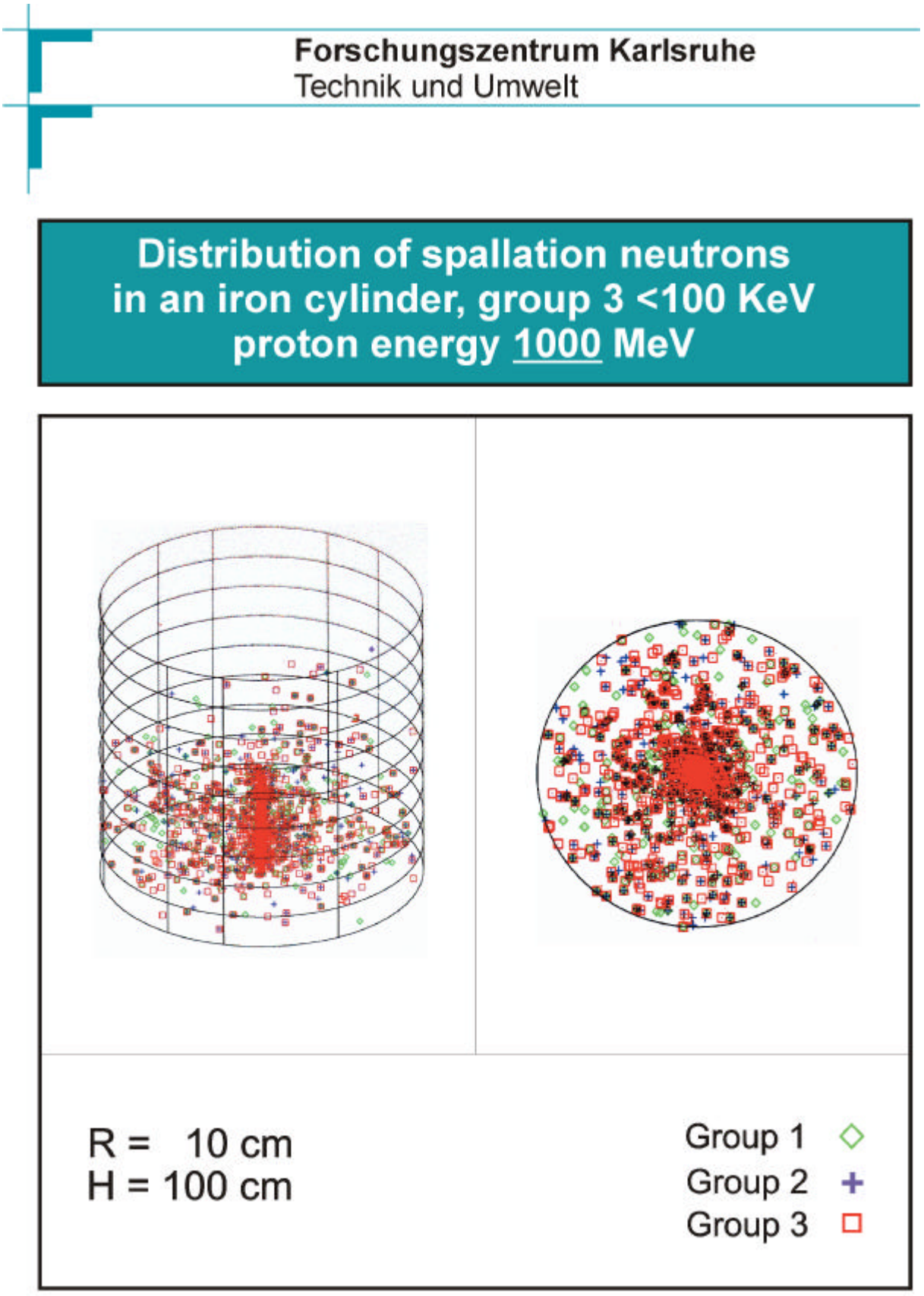

Figure 2: Neutron distribution in an iron cylinder by irradiation with 1000 MeV protons

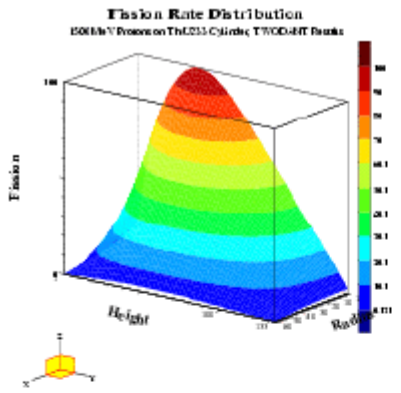

Proton hits target at the bottom of the core

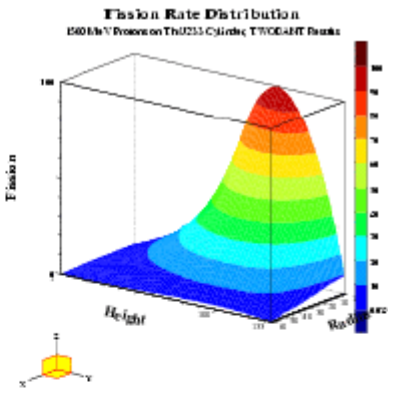

Proton hits target at the coremidplane

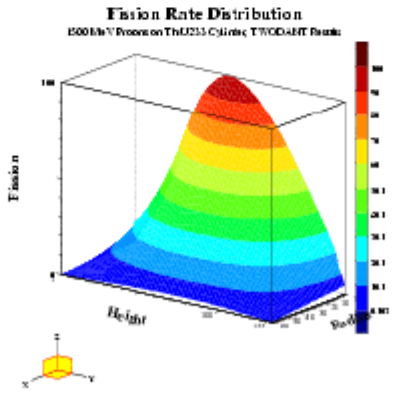

Proton hits target 30cm above bottom of the core

Figure 3: Fission rate distributions for three impact points of a 1500 MeV proton beam

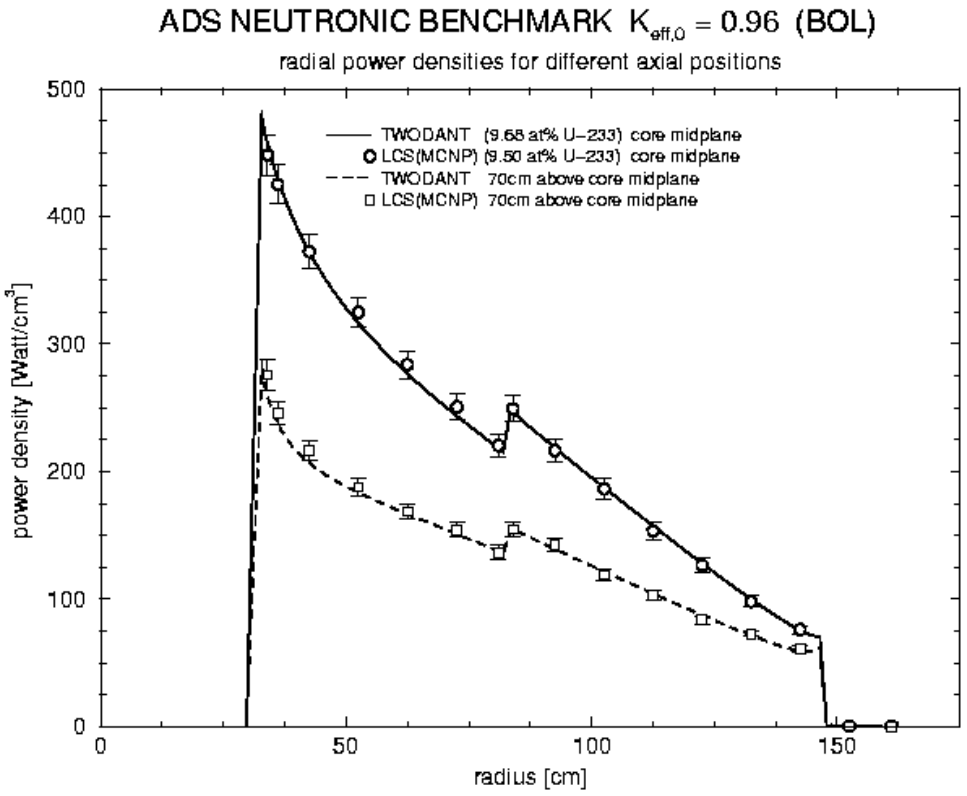

Figure 4: Comparison of radial power density distributions for the IAEA benchmark from TWODANT and MCNP calculations

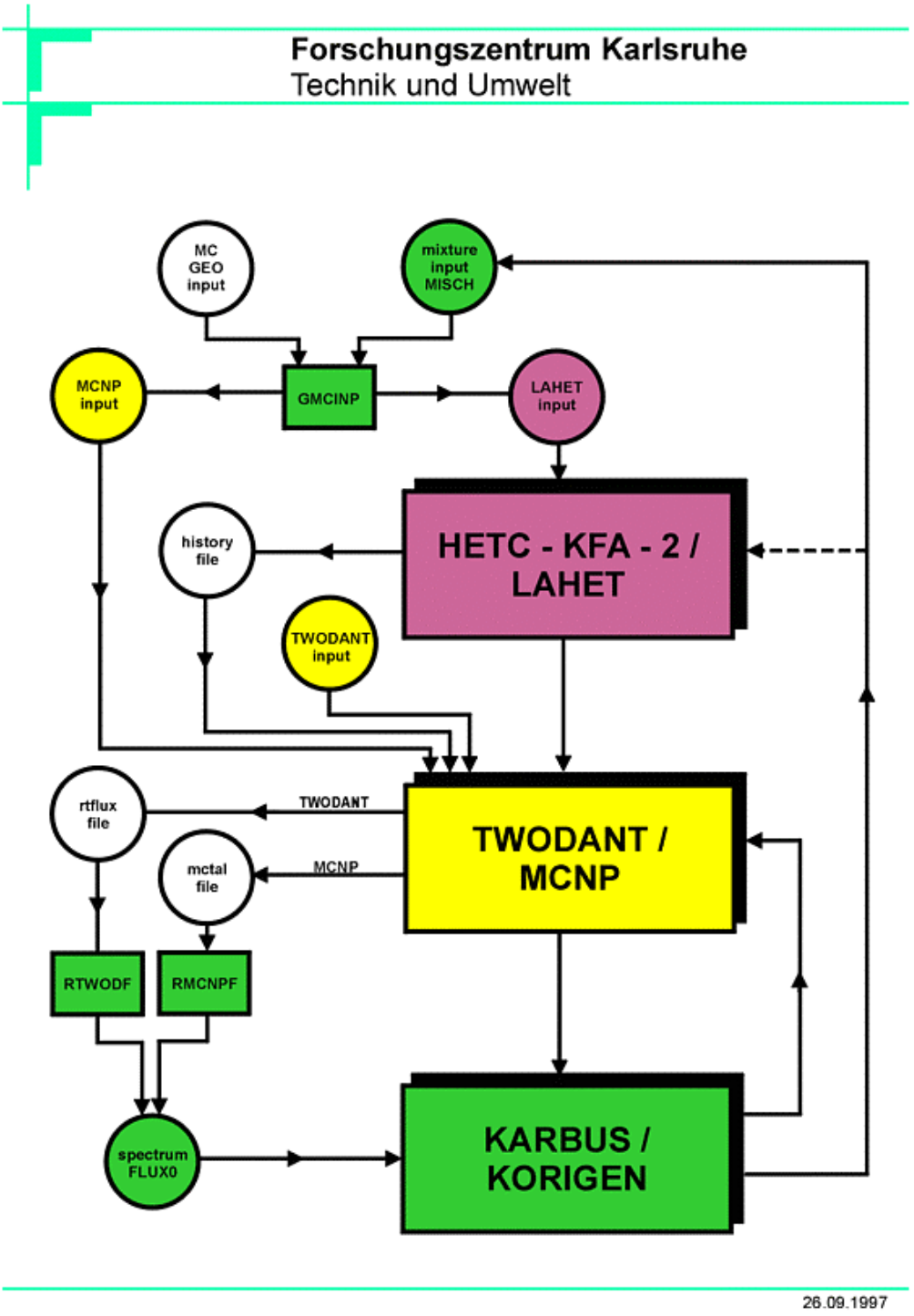

Figure 5: Detailed flowchart for a complete ADS calculation at FZK

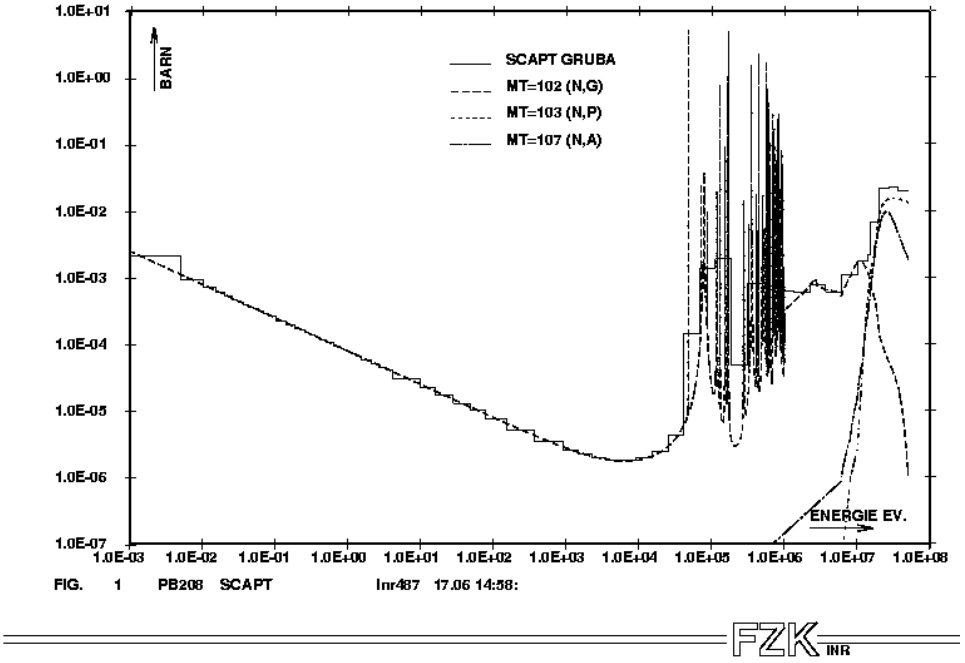

Figure 6: Comparison of point- and groupwise cross sections of lead

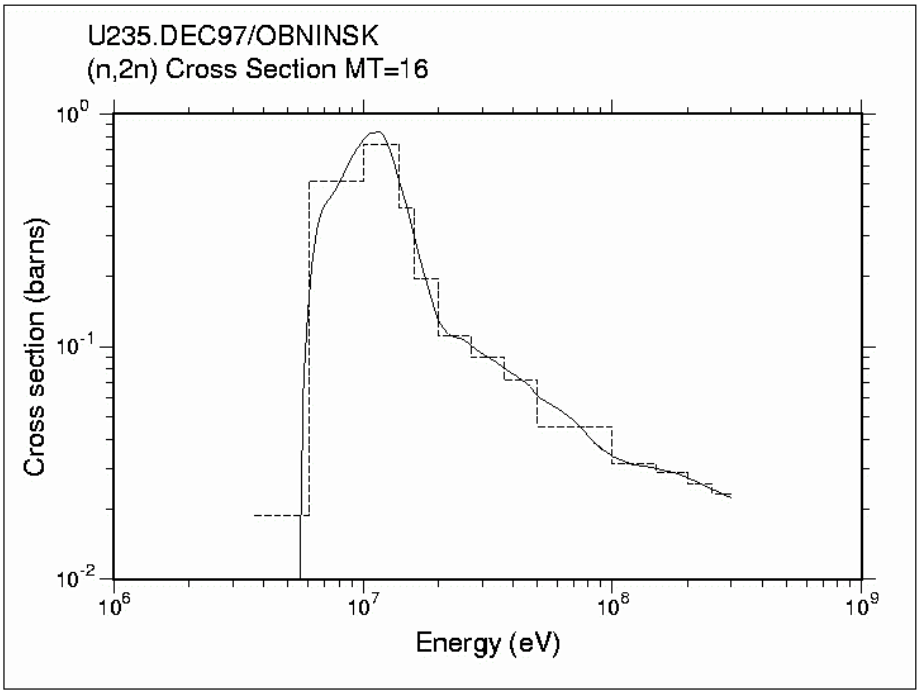

Figure 7: Comparison of point- and groupwise cross sections of U^{235} with NJOY

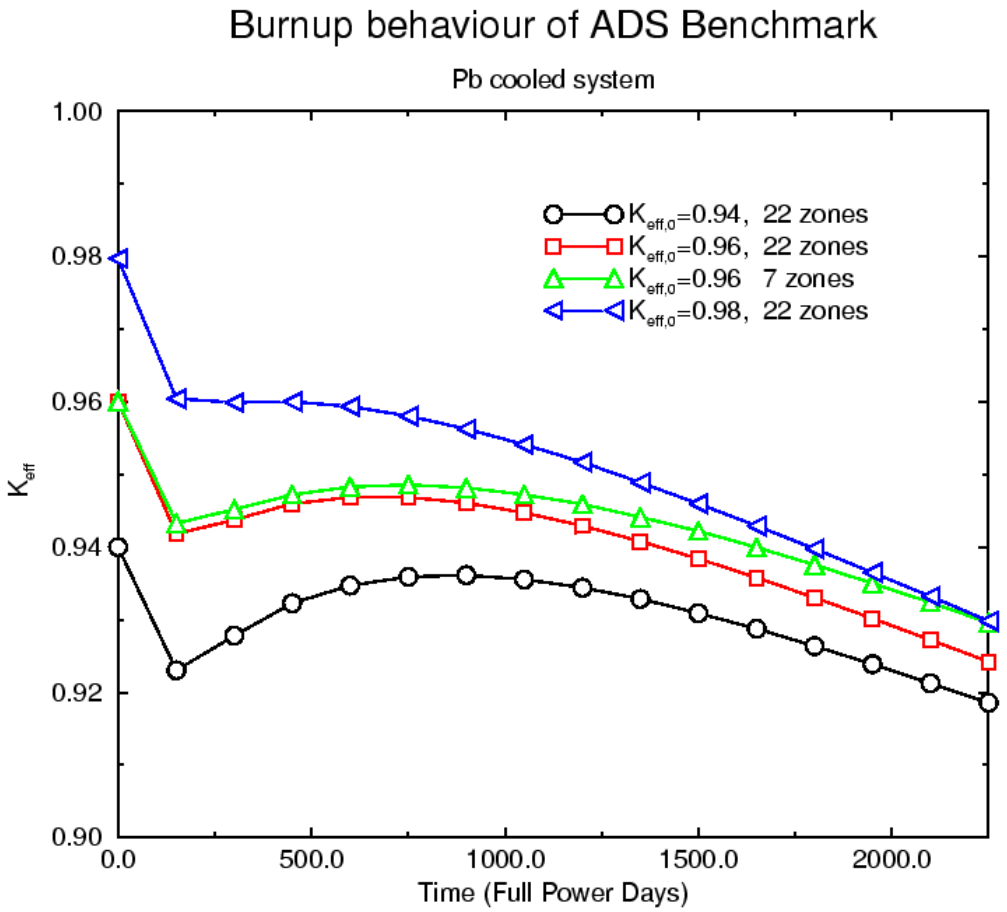

Figure 8: Reactivity of the IAEA ADS benchmark as a function of full power days

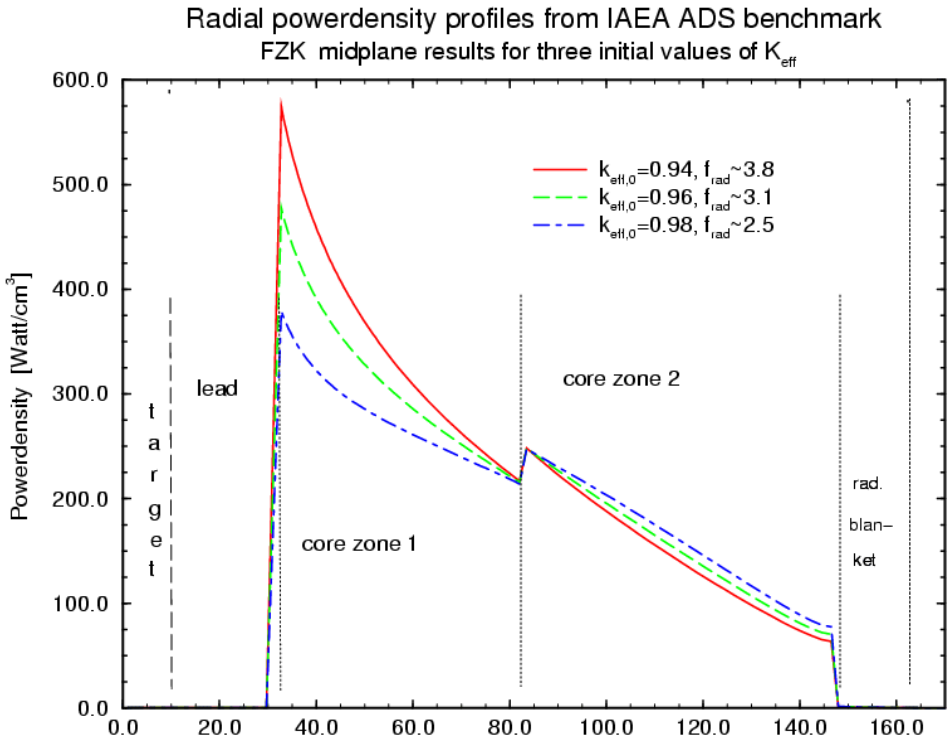

Figure 9: Comparison of radial power density distributions for the IAEA benchmark for three initial values of K_{eff}.

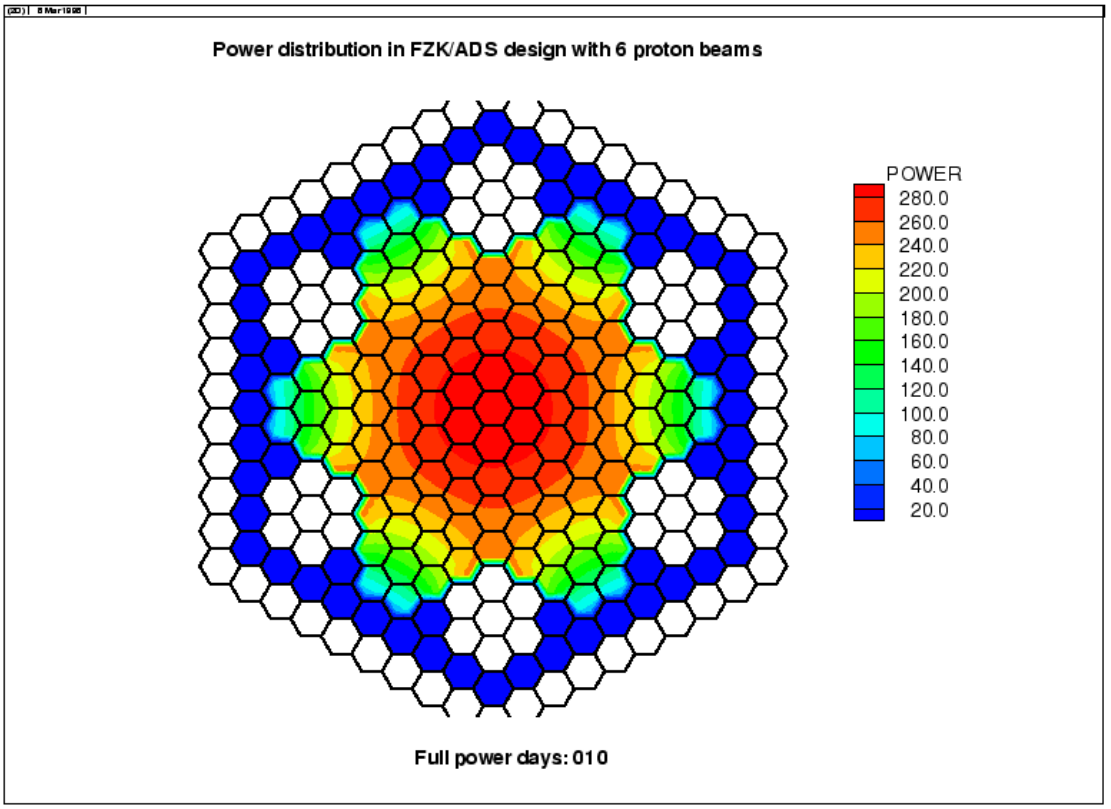

Fig 10: Power density distribution in an ADS with 6 proton beams

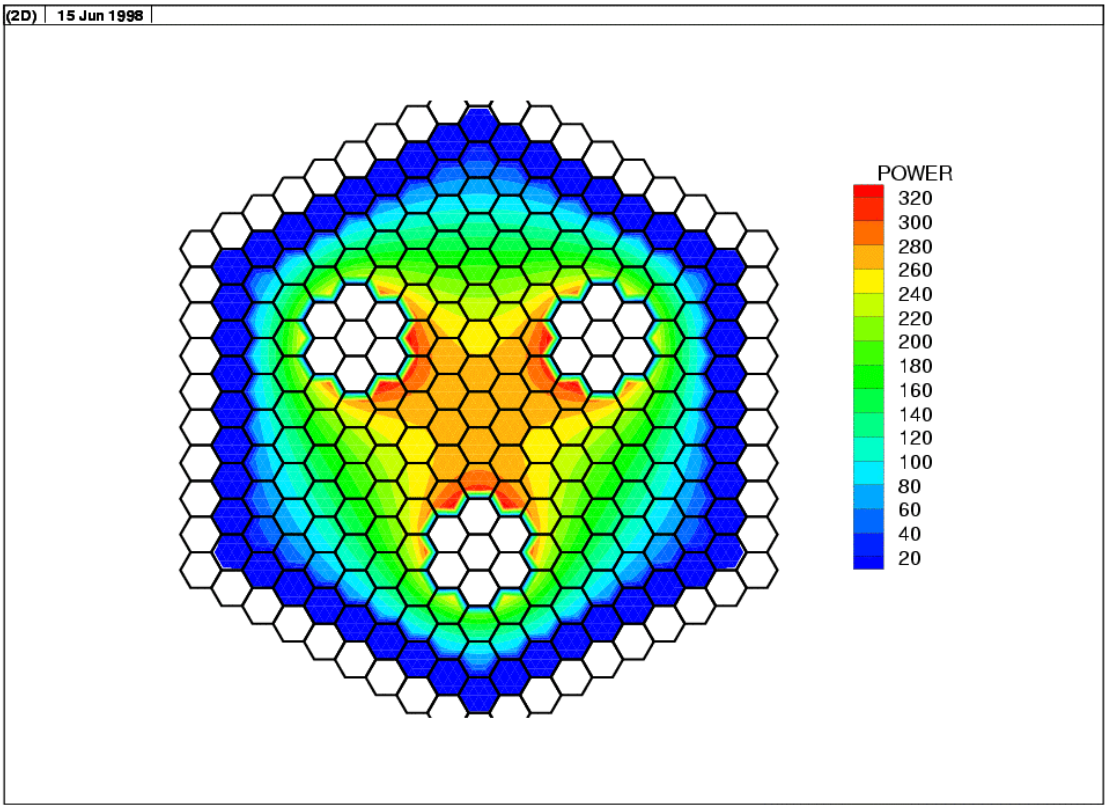

Fig 11: Power density distribution in an ADS with 3 proton beams

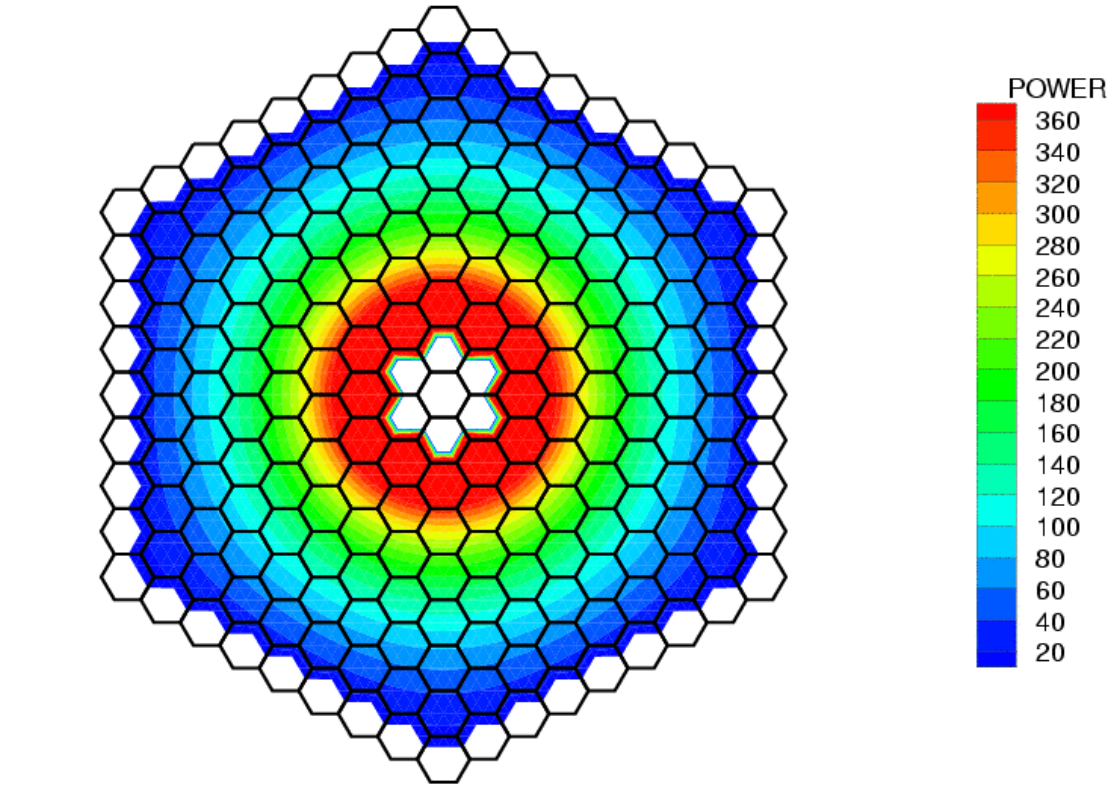

Figure 12: Power density distribution in an ADS with central proton beam

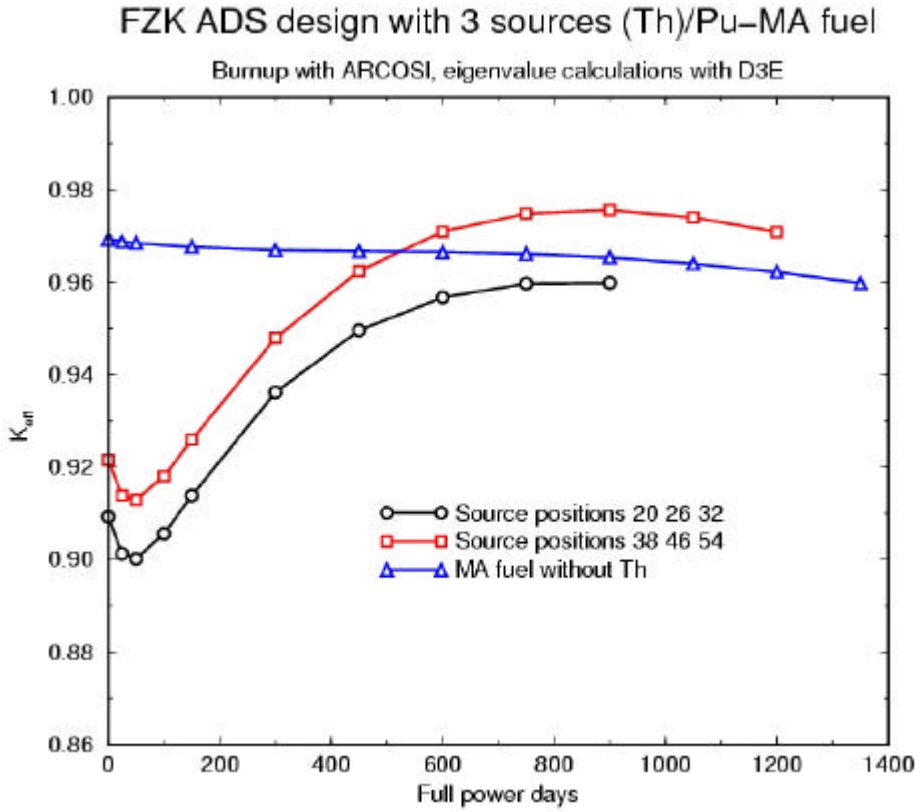

Figure 13: Time dependence of the reactivity of an ADS with different fuels

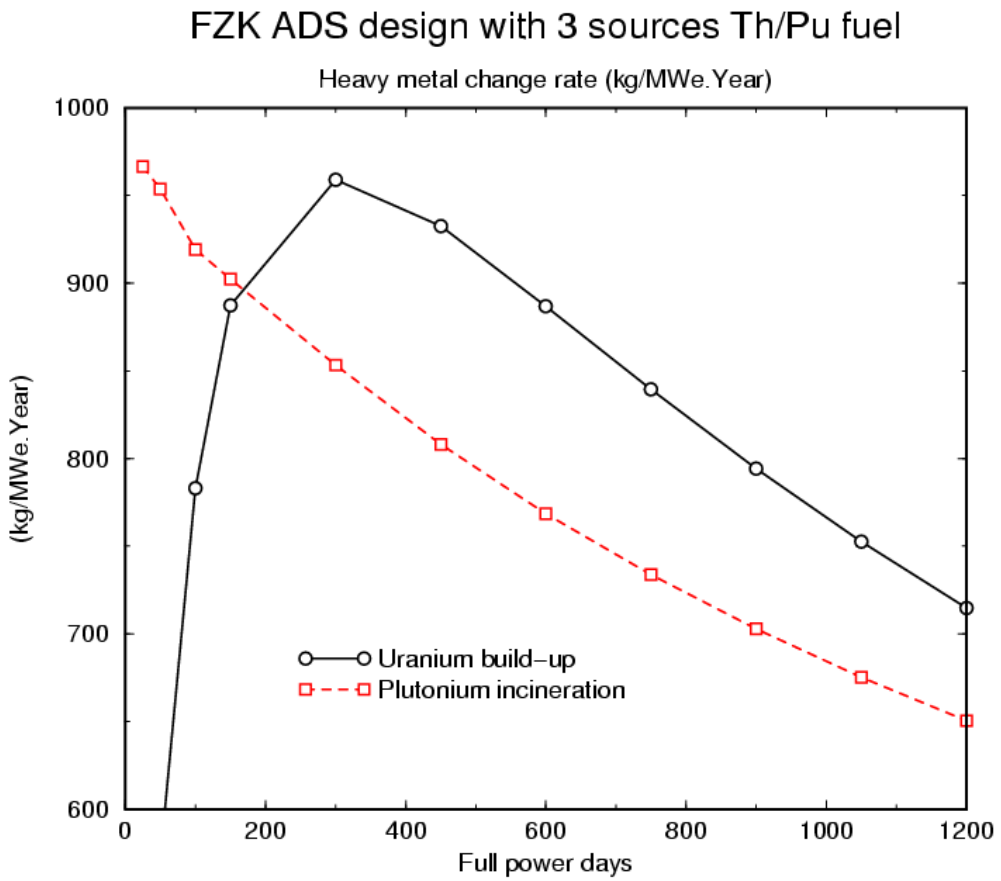

Figure 14: Change rates of uranium and plutonium in a lead-cooled ADS with 3 proton beams

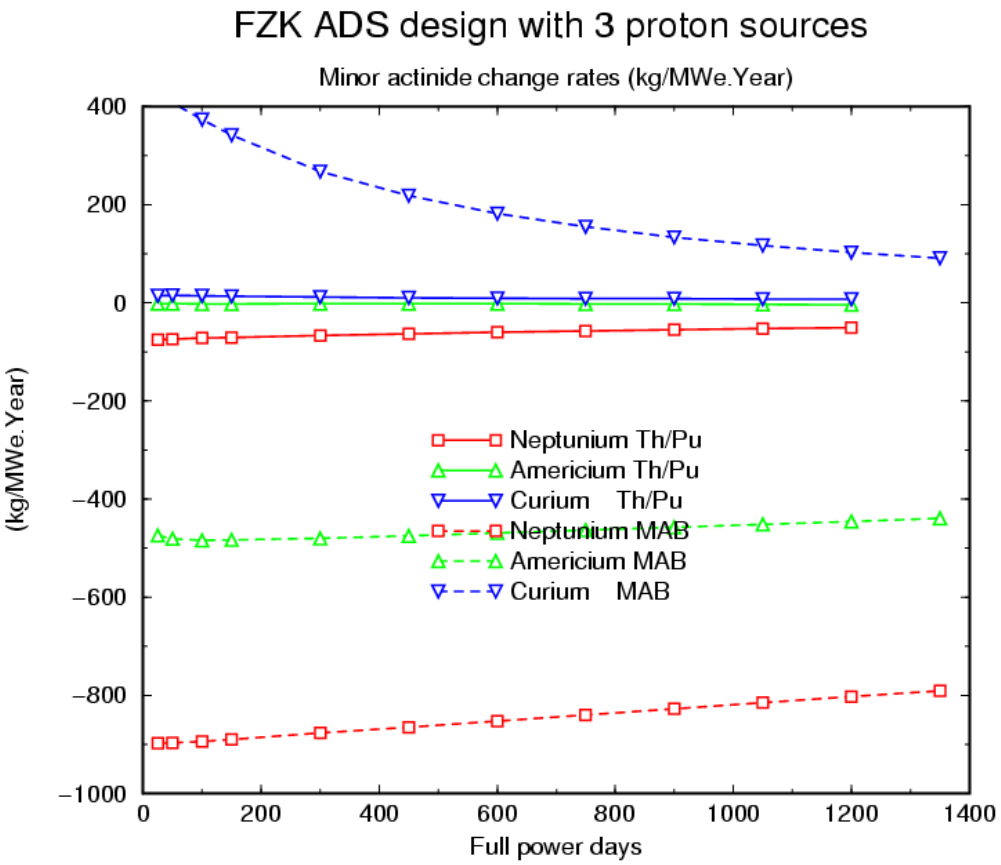

Figure 15: Changes of minor actinides in a lead-cooled ADS with 3 proton beams

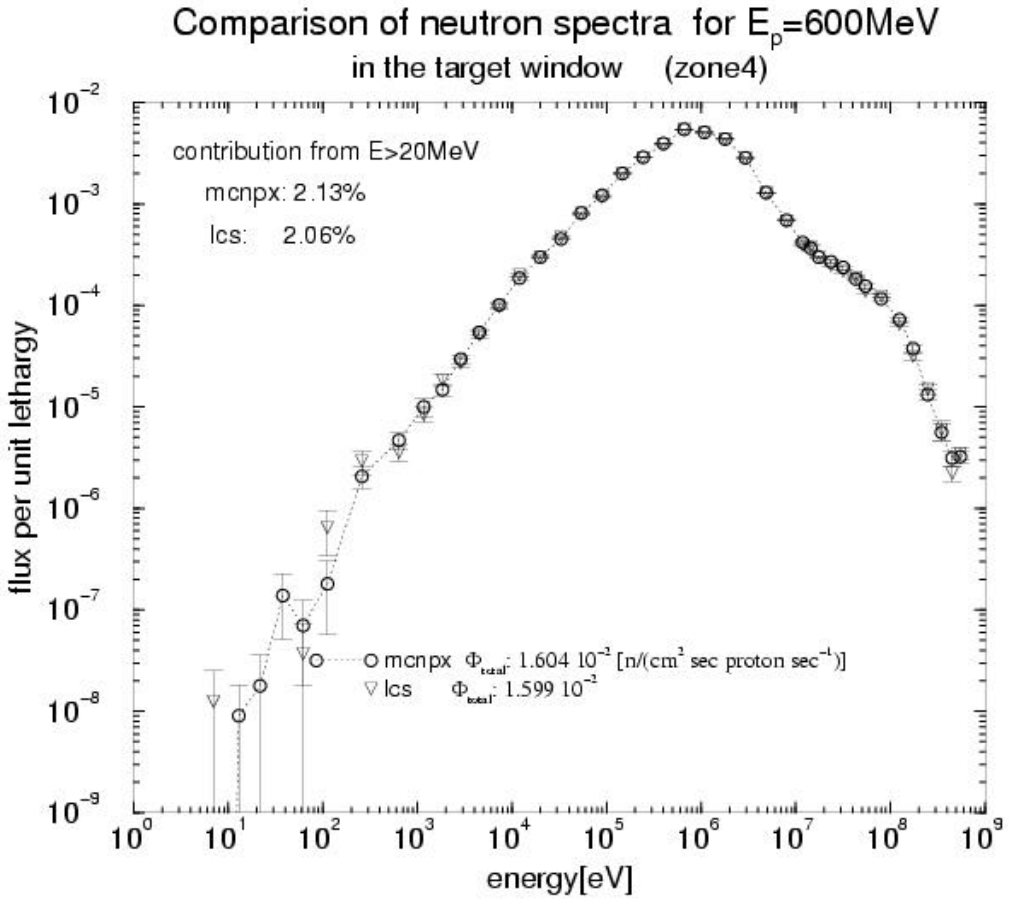

Figure 16: Comparison of neutron spectra from MCNPX and LCS in a target window

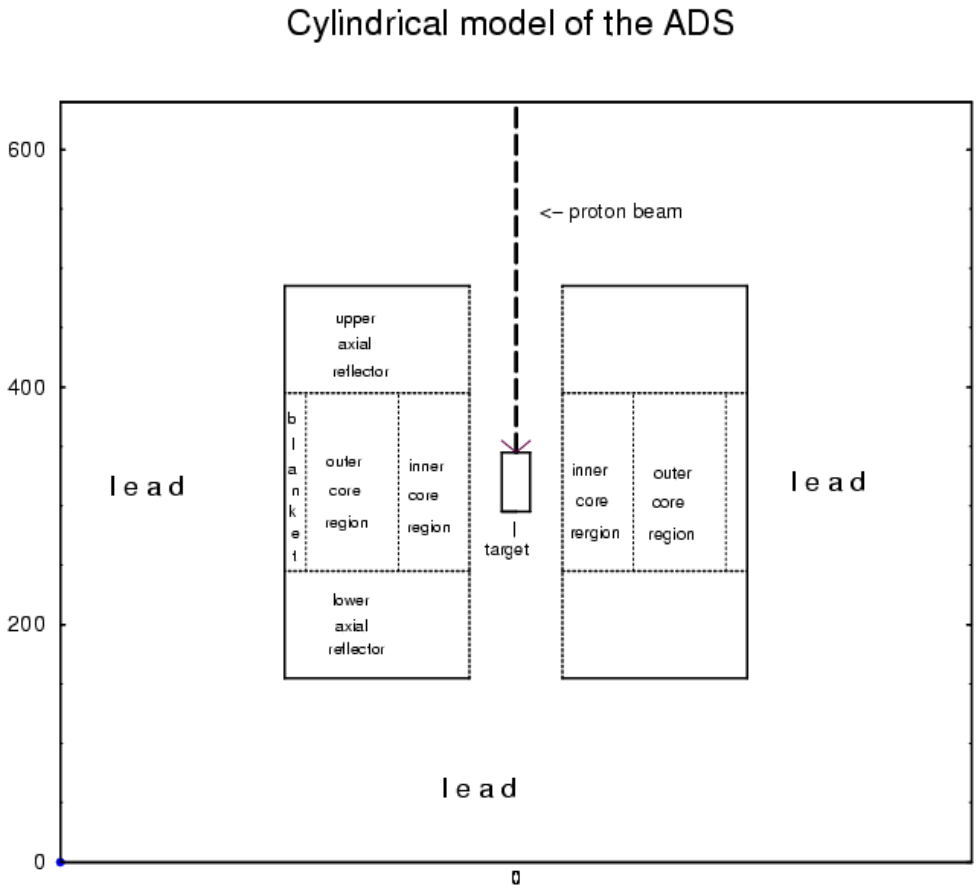

Figure 17: Cylindrical model for the ADS target and spallation product investigations

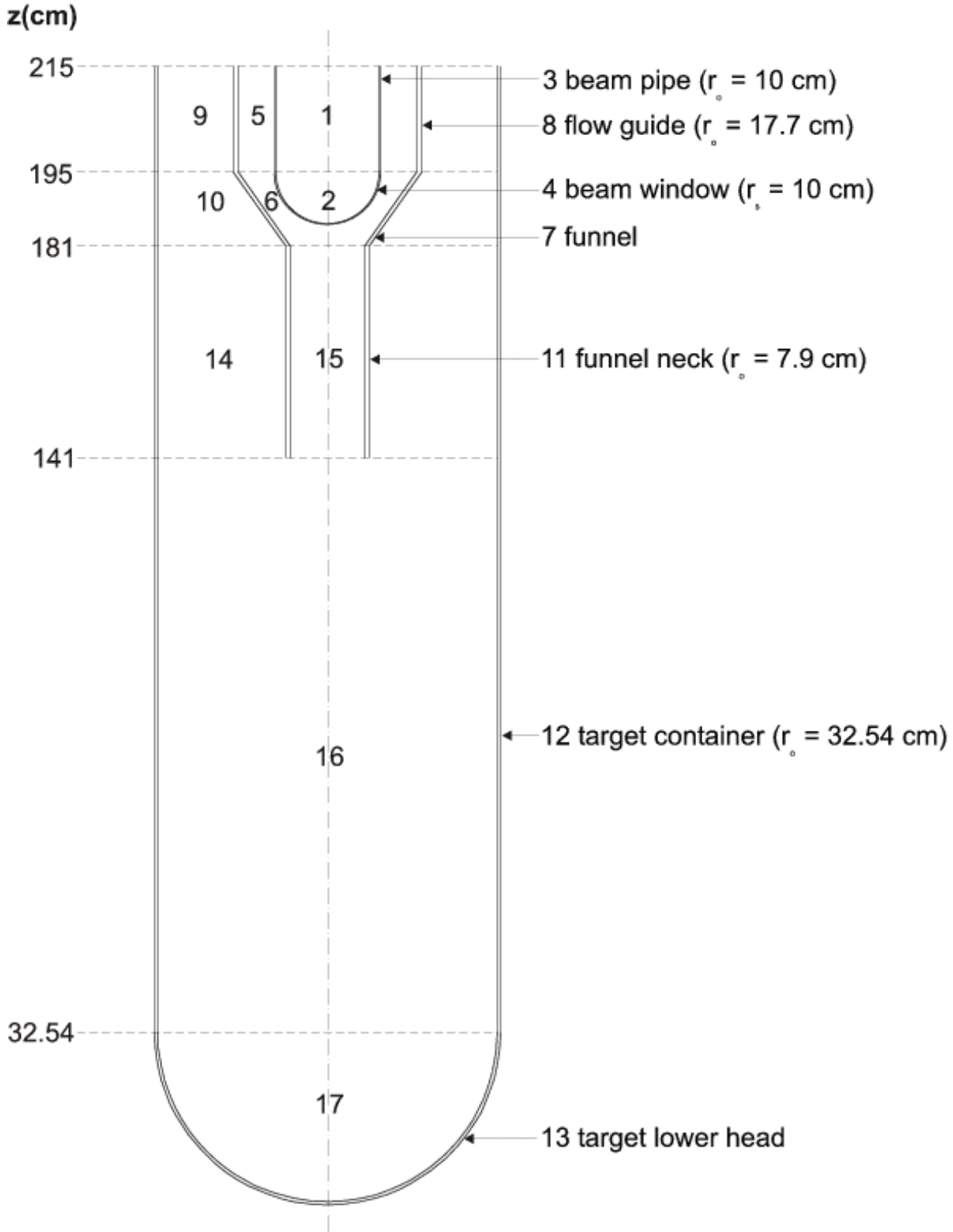

Figure 18: Geometry model of the target used for the calculations with the LCS code

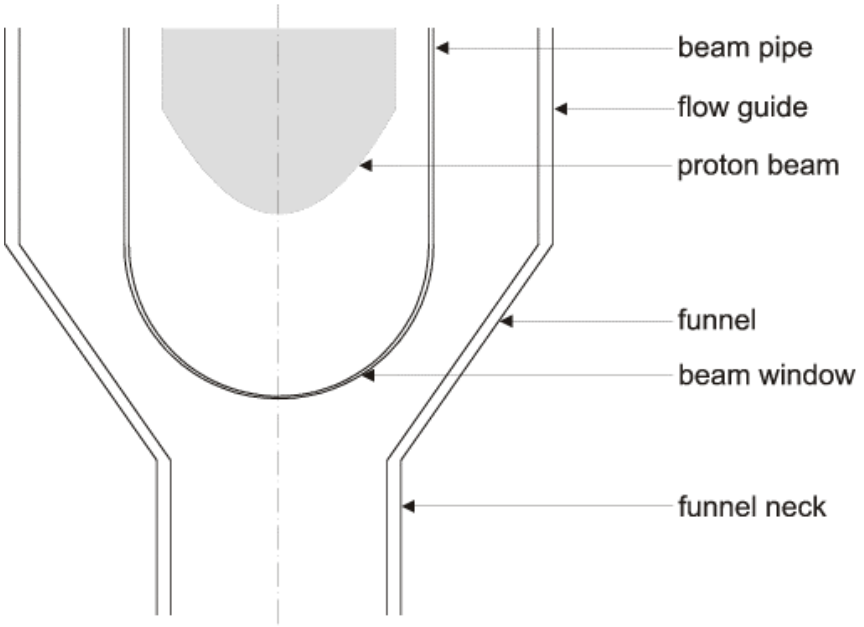

Figure 19: Geometric model of the target in the vicinity of the window

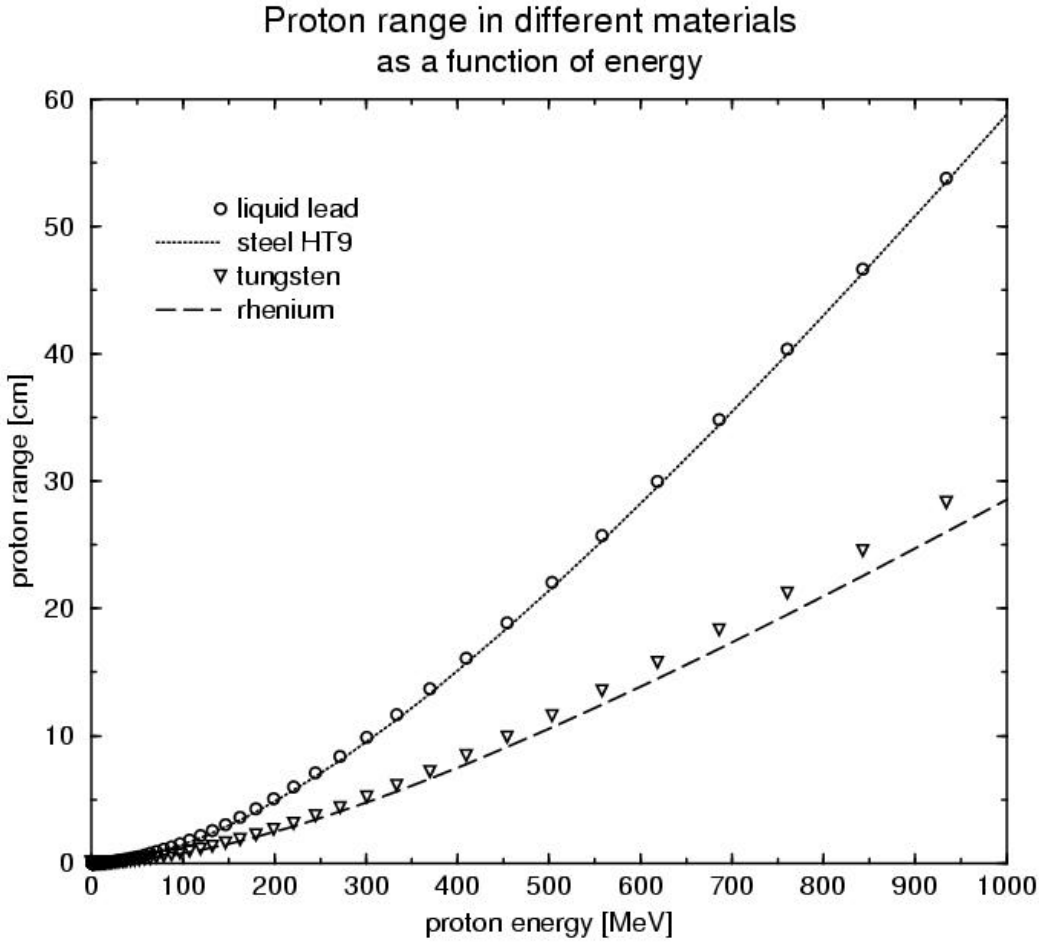

Figure 20: Proton range in different materials for proton energies up to 1000 MeV

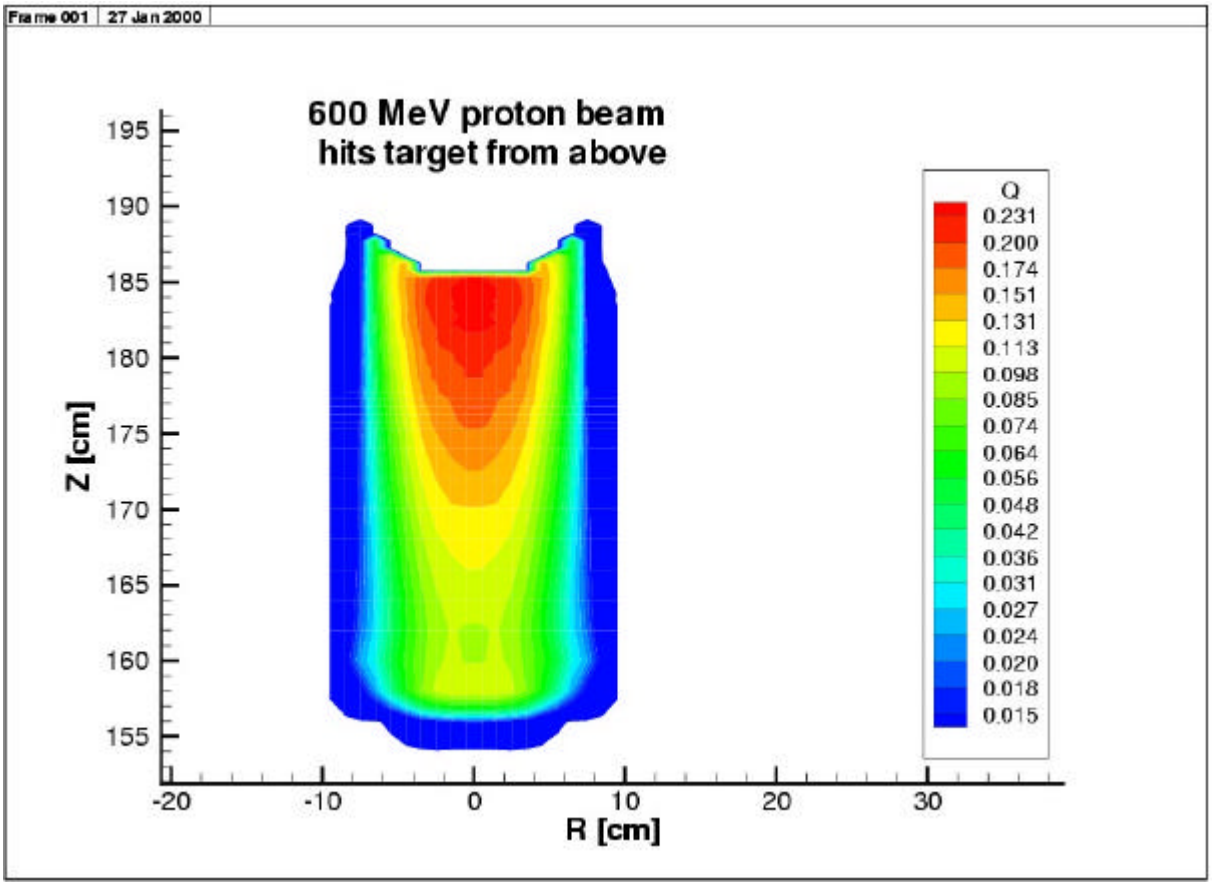

Figure 21: Energy [kW/mA$\bullet$cm^3] deposited in a liquid lead target by a 600 MeV proton beam